HERMETIC GAS FIRED RESIDENTIAL HEAT PUMP

David M. Berchowitz, Director and Yong-Rak Kwon, Senior Engineer
Global Cooling BV, Ijsselburcht 3, 6825 BS Arnhem, The Netherlands
Tel: 31-(0)26-3653431, Fax: 31-(0)26-3653549, E-mail: info@globalcooling.com

ABSTRACT

The free-piston Stirling engine driven heat pump (FPSHP) is presented as an alternative residential heat pump technology. In this type of heat pump system the mechanical output of an externally heated free-piston Stirling engine (FPSE) is directly connected to a Rankine or transcritical cycle heat pump by way of a common piston assembly. The attractiveness of this system is the economics of operation when compared to an electrically driven conventional heat pump as well as the low environmental impact of the system. It is expected that the primary energy ratio for the ground water source FPSHP will be close to 2.15 for heating mode and 3.34 for cooling mode with the inclusion of domestic hot water generation. The working fluids are dominantly helium (He) gas for the engine and carbon dioxide (CO_2) for the heat pump. Technical concerns for this system include the effects of working medium mixing and the load stability under various operating conditions. The direct connection of the Stirling engine to the compressor of the heat pump allows for the working fluids to mix with each other. He separation for the heat pump is discussed and the effect of the mixing of working fluids on both the heat pump and Stirling engine is investigated through a demonstrative experiment and simulation. Experimental verification of the performance due to the mixed working fluid is presented for the heat pump cycle, while simulation techniques with proper gas mixture properties are used to determine the effect on the Stirling cycle. About 50% by volume of CO_2 gas is expected in the working fluid of the free-piston Stirling engine and less than 1% by volume of He gas is expected in the CO_2 heat pump cycle.

Key Words: *heat pump, free-piston, Stirling, gas-fired, natural working fluid, CO_2 cycle*

1 INTRODUCTION

It is well known that fuel driven heat pumps allow far greater energy utilization. This is measured by the primary energy ratio (PER), which is defined as the ratio of useful energy provided by the device divided by the original generated energy needed for input. For example, the PER of an electric heater is just the fraction of energy originally consumed as fuel at the central electric generating facility that is made available as electricity at the point of use. Usually about 0.38. An electric heat pump has a much higher PER since it adds energy taken from the environment to the input to provide the heat output. In this case the PER may be above 2.0 for a ground water heat pump. A fuel driven heat pump has the highest potential PER in that by utilizing the primary energy source on site, it is able in theory to capture all the heat of conversion to provide that in addition to the pumped heat. The PER in this case may approach 2.5 with the additional advantage that primary energy is generally cheaper on a per unit energy cost basis.

Gas fired heat pumps using the Stirling as the prime mover has been pursued many times before. Efforts include a Duplex Stirling arrangement by Sunpower in 1983 (Penswick and Urieli 1984), a free-piston Stirling engine hydraulically driving a Rankine heat pump by Mechanical Technology Inc. (Marusak and Ackermann 1985), a second and third effort by Sunpower using an inertial drive and magnetic coupling to a Rankine heat pump (Wood et al. 2000, Chen and McEntee 1993) and various efforts in Japan (MITI 1986) and Europe (Lundqvist 1993). All these efforts identified the obvious advantages of the Stirling engine being its high part load efficiency coupled with a potential for high reliability and long life. However, in every case, these efforts failed in their approach to coupling the Stirling engine to the heat pump in a practical cost-effective manner. The concept laid out here offers a

simple technique that allows direct coupling to a Rankine heat pump while preserving all the virtues of the free-piston Stirling engine.

Unlike previous work, no effort is made to completely isolate the working fluid of the engine from the heat pump. The FPSHP utilizes a He–CO_2 mixture for its working fluid and some intermixing is allowed to occur. The engine will operate well with concentration ratios of CO_2 to He of 100/0 to 50/50. On the other hand, the Rankine heat pump will be more strongly affected by the working fluid mixture and consequently a He separator must be employed. Since the state of the CO_2 is at one point in the cycle almost entirely liquid, it is relatively easy to separate out the He and return it to the engine thereby keeping the Rankine working fluid almost entirely free of He. The net result is that the engine operates with a He–CO_2 mixture while the heat pump operates with an almost pure CO_2 cycle.

The device detailed here has been sized for residential applications using a ground water source/sink for one end of the heat pump cycle. The CO_2 cycle never goes transcritical and therefore COP is maintained at high levels under all load conditions. Pressures also remain relatively low compared to the standard CO_2 transcritical cycle.

The use of CO_2 has a number of strong attractions. It is identified as a 'natural' working fluid and as such is seen as relatively benign to the environment. In the application of a ground water heat pump, its operation is always below the critical point which greatly simplifies the implementation of the cycle. For the particular machine discussed here, CO_2's high dissociation temperature (in excess of 1500 K) and transport properties, make it far less detrimental to the performance of the Stirling engine even in relatively high proportions to the He charge.

2 SYSTEM DESCRIPTION

The FPSHP system has been configured for use with a ground water source/sink in order to maximize the energy utilization per unit input, as shown in Fig. 1. The system is composed of two major sub-systems: the FPSE and the CO_2 heat pump. The FPSE is composed of a combustor and a Stirling engine. The CO_2 heat pump is composed of typical Rankine cycle components with the addition of the He separator. A control system not shown in the Fig. 1 is required for load matching between the FPSE output power and compressor power for the Rankine cycle. Total estimated mass of the FPSHP but not including external heat exchangers and auxiliaries is 18 kg.

Heat transport to indoor spaces could be by secondary water or air circulation. The energy source for the external combustion system most readily available in residential areas would be natural gas. For a completely autonomous system, additional power could be provided from the FPSE alternator/motor to power the peripheral components such as water circulation pump, indoor fan, burner blower, and electronics. Two 4-way valves are necessary to switch the heating and cooling mode of the heat pump. Rejected heat, from the FPSE, can be recovered and utilized, either by a storage tank to augment domestic hot water production or by direct integration into space heating. Waste heat of combustion is used for super-heating CO_2 vapor entering the suction process. This is done in order to increase the heat pump discharge temperature and promote heat transfer in heating mode. The CO_2 cycle remains sub-critical for all conditions during the heating mode. Therefore, there are four possible modes of operation: indoor heating, indoor heating plus water heating, water heating, and indoor cooling plus water heating.

Since CO_2 leakage across the compressor piston to the engine side increases the engine mean pressure, the He–CO_2 mixture returns to the compressor by a return device that is activated by pressure difference between engine mean pressure and compressor suction pressure. He out of the mixture returned into the compressor side is separated by the He separator. The He separator located at the end of condensation and sub-cooling process separates He gas and returns it to the engine side. If the CO_2 cycle goes to a transcritical cycle, the He separator can be located after a partial expansion with an additional

expansion device (not shown in Fig. 1) to force the refrigerant into a complete liquid state. The mean pressure of the FPSE is the same as the CO_2 cycle suction pressure. As shown in Fig. 2, the suction pressure of the CO_2 cycle varies with evaporator operating condition. Therefore, the FPSE operates not only under different He–CO_2 mixtures but also at the different mean pressures.
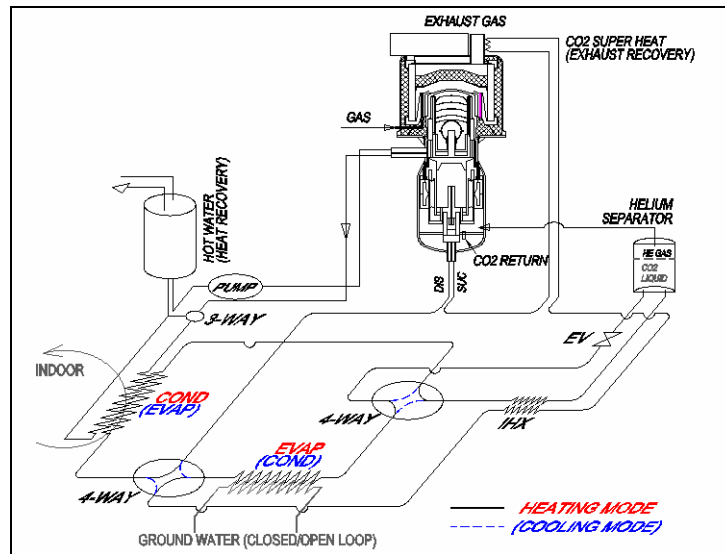
Figure 1: Layout for the free-piston Stirling engine driven heat pump using ground water.

2.1 Operation and Design Condition

A direct comparison of efficiency between the FPSHP and existing heat pumps is not such a simple task because system efficiency and capacity varies with the test standard (Payne and Domanski 2001). This study uses the test standard of ISO 13256-1 for performance calculation and the efficiency status provided by the US DOE Energy Star program for performance comparison. The ISO 13256-1 defines three applications: water loop (WLHP), ground water (GWHP), and ground loop (GLHP). This study discusses a ground water heat pump system (GWHP) that is hermetically connected to the FPSE. Table 1 shows the operating conditions and the efficiency status for a ground source heat pump system (GSHP). The Energy Star recommended COP can be converted to PER by multiplying by 0.38 (the assumed electricity generation and transmission efficiency). Therefore, the converted PER for the Energy Star recommendation for the GWHP is 1.79 and 1.37 for cooling and heating respectively. Cooling and heating capacity is around 10 kW for these examples.

Table 1: Test condition for GSHP by ISO 13256-1 and efficiency status by the US DOE.

Operation	Description	GWHP	GLHP
Cooling	Air entering indoor unit – DB/WB	27°C/19°C	27°C/19°C
	Water entering	15°C	25°C
	Energy Star recommended EER(COP) *	16.2 (4.7)	14.1 (4.1)
Heating	Air entering indoor unit	20°C	20°C
	Water entering	10°C	0°C
	Energy Star recommended COP *	3.6	3.3

* US DOE: http://www.eere.energy.gov/femp/technologies/eep_groundsource_heatpumps.cfm

The operating condition for the FPSHP component design is summarized in Table 2. The FPSHP component design, presented here, takes into consideration a potential requirement for supplemental water heating in case the FPSE's heat rejecter temperature is not high enough for domestic hot water storage/use. For complete water heating without backup electric heaters and/or a transcritical CO_2 cycle, a different design strategy could be applied with consideration of a general CO_2 heat pump operating strategy (Bullard and Rajan 2004). Condenser and evaporator designs are assumed to use a microchannel

3

heat exchanger similar to other approaches (Park and Hrnjak 2004) with the exception of strong consideration given to maintaining the compressor discharge pressure below the CO_2 critical point. CO_2 cycle sub-cooling and super-heating can be accomplished by an internal heat exchanger and a ground water bypass while the super-heating can be further enhanced by recovering the waste heat of combustion. Fig. 2 shows the heating and cooling mode cycle on a p-h diagram of CO_2 based on the design condition in Table 2.

Table 2: Operating condition for the FPSHP system design.

Component	Description	Heating	Cooling
FPSE	Mean pressure (bar)	36.7	42.8
	Work output (W)	1,300	650
	Hot head temperature (°C)	630	630
	Heat rejecter temperature (°C)	60	60
	Heat reject pump power (W)	25	← same
	Air blower power for burner (W)	25	← same
	Burner capacity (W)	5,000	← same
	Operating frequency (Hz)	64	66
CO_2 cycle	Discharge temperature (°C)	78	46
	Condenser outlet temperature (°C)	27	22
	Sub-cooling (°C)	3	7
	Evaporator inlet temperature (°C)	2	8
	Suction pressure (bar)	36.7	42.8
	Super-heating (°C)	28	12
Indoor HX	Air inlet temperature (°C)	20	27
	Air outlet temperature (°C)	40	17
	Fan power (W)	150	← same
Water HX	Water inlet temperature (°C)	10	15
	Water outlet temperature (°C)	5	20
	Pump power (W)	100	← same
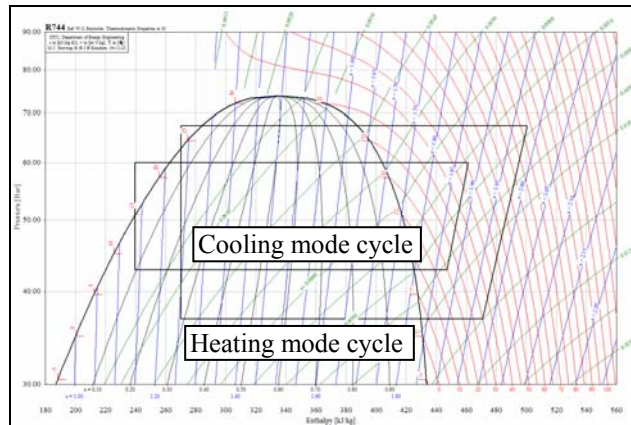
Figure 2: CO_2 p-h diagram for heating and cooling mode assuming a ground water-source heat pump.

2.2 Performance Estimation

In compliance with the test standard ISO 13256-1, the input energy for performance calculation includes a ground water circulation pump, a FPSE heat reject water pump, and a burner air blower. The indoor fan power is addressed separately. The test standard considers the indoor fan power together with the delivered energy to the indoor environment, and then it is credited for both delivered and input energy because it increases heating capacity and decreases cooling capacity. However, this study does not consider the indoor fan power. For the FPHSP system performance, the input energy is based on the primary energy, e.g. lower heating value of gas. Therefore, the electric input energy for the pumps and blower was converted to the primary energy assuming 38% electricity generation and transmission

4

efficiency. Design heating and cooling capacity is 8.3 kW and 7.5 kW respectively with an additional water heating of 2.9 kW. Table 3 shows the summarized performance. The efficiencies are calculated based on a specific design for each individual component – combustor, FPSE, compressor, He separator, and CO_2 cycle. Details of the design are discussed below.

The estimated PER for the FPSHP, shows performance, better than the Energy Star recommendation for a GWHP by 57% for heating and 87% for cooling. The FPSHP shows better performance for both heating and cooling mode because the waste heat is completely recovered and the FPSE efficiency is favorable to a lower ambient temperature for the cooling mode unlike other gas engine driven heat pumps (Zhang et al. 2004).

Table 3: System performance calculated for a ground water source FPSHP

Component	Description	Heating	Cooling
FPSE	Fuel input, lower heating value of gas (W)	4,840	2,380
	Burner efficiency (%)	87	87
	Engine efficiency (%)	30	30
	Exhaust heat (W) *partly using for super heating	630	310
	Engine reject heat (W) *fully recovered	2,950	1,450
	Engine mechanical power (W)	1,260	620
CO_2 cycle	Compressor power (W)	1,260	620
	Compressor overall efficiency (%)	90	91
	Cycle COP: ideal COP x compressor efficiency	6.57	12.18
	Condensation (W)	8,300	9,000
	Evaporation (W)	7,700	7,500
System performance	Delivered/removed energy to/from indoor (W)	8,300	7,500
	Delivered energy to water heating (W)	2,950	1,450
	PER with consideration of 2 pumps & burner blower	2.15	3.34

3 INVESTIGATION OF STIRLING ENGINE AND CO_2 CYCLE HEAT PUMP

Since the FPSHP is a hermetically sealed system and the working fluid is different for the FPSE and heat pump cycle, the He–CO_2 mixture is to be managed for optimal performance. The operating characteristics, associated with the He–CO_2 mixture are presented for the FPSE. A CO_2 cycle analysis with the compressor and an experiment for He separation using a R134a demonstrative cycle were conducted. It is inevitable to have He and CO_2 mixing together in both the FPSE and heat pump cycle. By means of the He separator and CO_2 return device, CO_2 concentrations in the FPSE and He concentration in the heat pump can be controlled. The higher the He fraction in the FPSE, the more He flows in the heat pump cycle. This situation improves the FPSE efficiency and reduces the volumetric efficiency in the heat pump cycle. Since He gas in the heat pump cycle also affects the discharge pressure of the compressor, there is an optimum fraction for each gas in the mixture. Without in-depth analysis for the optimum mole fraction, this study assumes 0.5 as a minimum CO_2 fraction in the FPSE volume because this condition makes the He volumetric flow rate in the heat pump cycle equal to the CO_2 volumetric leakage rate across the compressor piston (this amount of He flow in the heat pump cycle is predicted to have an insignificant effect on the CO_2 cycle performance).

3.1 Free-piston Stirling Engine (FPSE)

The FPSE utilizes a closed regenerative cycle in a power producing mode. Heat input to the engine is by external combustion thus in principle allowing different energy sources though in this study only natural gas is considered. The free-piston configuration employs the variations of the working gas pressure to drive mechanically unconstrained reciprocating elements. As a consequence, the following important advantages arise:

a. There are negligibly small side loads on the moving parts thus removing the need for liquid lubricants. Typically, gas bearings are used which lead to long operating lives.
b. There is no requirement for an external dynamic high-pressure seal to the environment since the machine is hermetically sealed.
c. Having only two internal moving parts allows for compact simple construction. The first is the displacer, which is responsible for moving the working gas at constant volume between the compression and expansion spaces. The second is the piston, which compresses the working gas when it is in the cold side (compression space) of the machine and expands it when it is in the hot side (expansion space) of the machine. These components are shown in Fig. 3 (left).
d. Relatively simple power modulation by changing the amplitude of the mechanically unconstrained piston. This leads to significant off design-point energy savings.

A more complete description of the FPSE workings may be found in the following reference (Redlich and Berchowitz 1985).

Typical indicated efficiencies in the 1 kW class of He charged machines lie in the range of 30 to 35% (Lane and Beale 1997). An example of such a machine recently developed by Sunpower Inc. for home micro-cogeneration applications is shown in Fig. 3 (right). In the application treated here there is a mixing of the heat pump and engine working fluids and this tends to slightly depress the maximum available efficiency by about 10% for a 50/50 mixture of CO_2 and He. Aside from this, the efficiency is mainly limited by the maximum hot-end temperature and minimum cold-end temperature. For residential applications, the limits of delivered hot water temperature set the bounds of the cold-end to about 60°C while corrosion and creep restrict the hot-end to about 630°C for austenitic stainless steels. Alternative materials for the hot-end may allow higher temperatures and consequently improve efficiencies (Marusak and Ackermann 1985 report using Inconel 713 at 735°C).
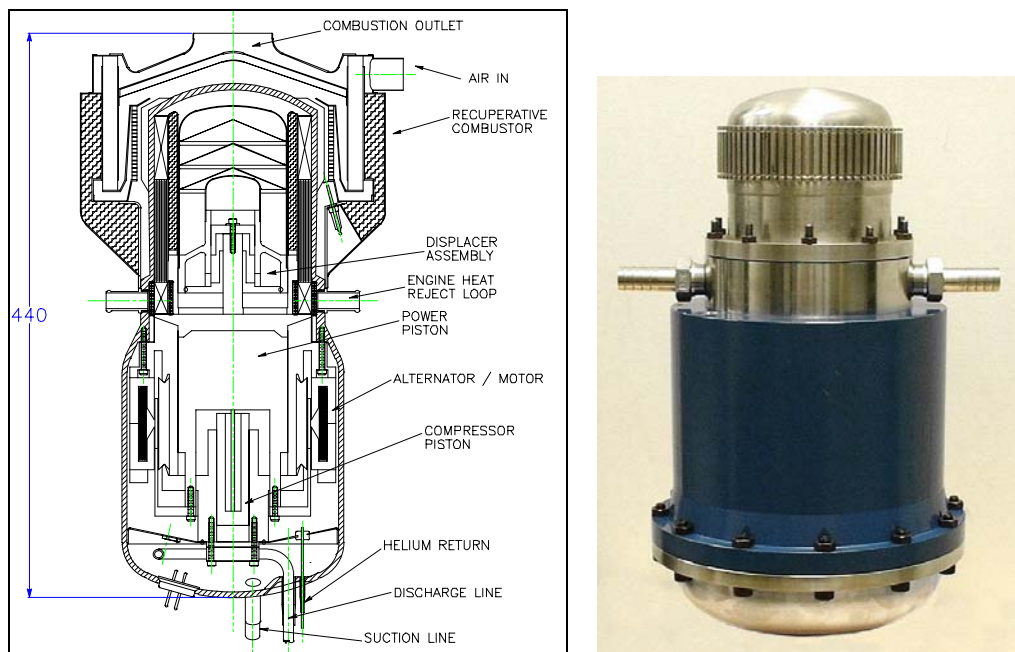
Figure 3: Preliminary design of FPSE for FPSHP system (left) and prototype FPSE 1kWe generator (right)

3.1.1 Combustor

The combustion process is located close to the head of the Stirling to ensure rapid quenching of the flame in order to limit NO_x formation. Many small jets in a ceramic flame holder provide for mixing of the fuel and air. The exhaust gas is led to a folded fin counter flow heat exchanger operating as a recuperator for the incoming air. Overall efficiency based on the lower heating value is expected to be

better than 85%. A maximum efficiency of 92% is deemed possible. In this case the combustor would be condensing and therefore this efficiency would be based on the higher heating value. A turn down ratio of at least 5:1 is needed to accommodate the load range expected of the system. A preliminary layout of the combustor is shown in Fig. 3 (left).

3.1.2 Engine operating characteristics

For other parameters fixed, a FPSE power is approximately proportional to the square of the piston amplitude as shown in Fig. 4. This presents some difficulties in load matching since the compressor input power is directly proportional to piston stroke. In case (a) in Fig. 4, it is clear that the compressor would draw more power than the engine is capable of supplying up to a stroke where the two curves intersect (point A). Thus at any stroke condition below this intersection, the engine would stall under the compressor load. Once the stroke exceeds the point where the powers intersect, the engine will provide more power than is possible for the compressor to absorb. Under this condition the engine will increase amplitude until it collides with its mechanical limits. Clearly this situation is unstable for all conditions of load and power. In case (b), the compressor load curve has a dead band and intersects the engine power curve at two points. Point B is a positively stable intersection since as stroke increases the load increases forcing the engine to reduce stroke while below this point the engine has more power than the load allowing it to increase its stroke until it reaches point B. Therefore, in order to ensure load matching, a linear alternator/motor of a maximum power capability of some 350 W is mounted between the engine and the compressor (see Fig. 3). This device may either add or extract power up to its rated maximum. The load shape of the alternator/motor curve may be made steep enough for positive stability under all operating conditions as shown in Fig. 4 case (c). Note that the intersection point B is determined by the reflected load from the alternator/motor and may be placed at any point on the engine curve. For points where the compressor power is higher than the engine power, the alternator/motor simply provides the shortfall. Under normal steady operating conditions it is never expected that the alternator/motor will dissipate its maximum rated power. The alternator/motor is also the starter for the engine and is sized for an efficiency of 91%.
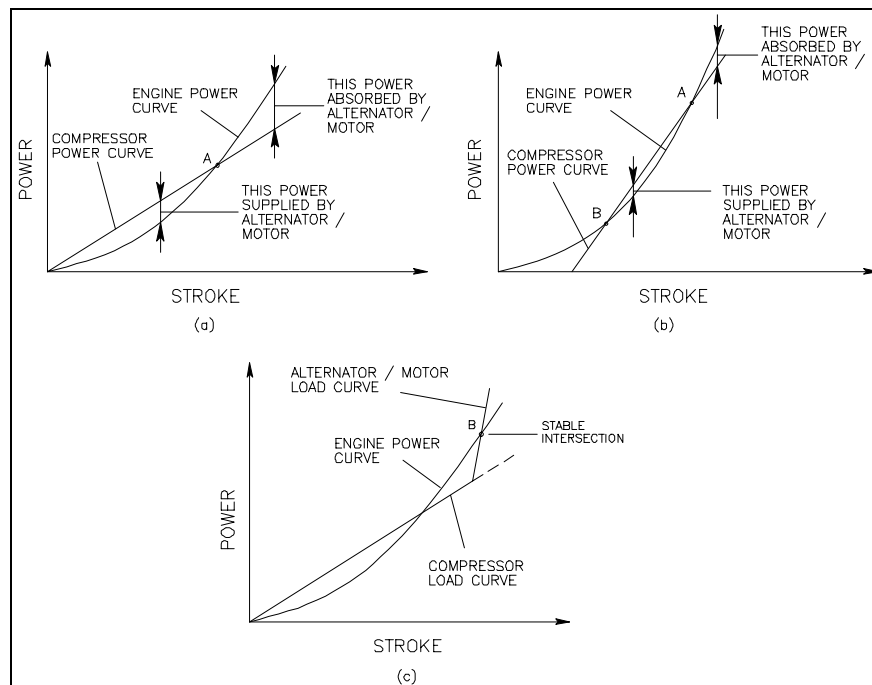
Figure 4: Power modulation with stroke

3.1.3 He-CO_2 mixture and performance analysis

Since the FPSHP operates at essentially the suction pressure of the heat pump (Fig. 1), the engine section must be able to offer satisfactory power and efficiency over all possible suction pressures. The two pressures representing likely limits of the suction pressure are estimated from the ISO 13256-1 standard for winter and summer operation using CO_2 as the working fluid. These are 36.7 bar (abs) for winter (heating) and 42.8 bar (abs) for summer (cooling) as shown in Table 2. Operation over such a broad pressure range results in an inevitable frequency change of about 5 Hz over the nominal 60 Hz. In order to retain engine tuning over this range of pressure, the displacer is resonated by a gas spring rather than the mechanical springs typically used. As the engine starts up, its working gas may be more dominantly CO_2. After a short while, the working gas mixture settles out to about a 50/50 mole mixture of CO_2 and He. In addition to this, the power must be modulated in order to meet the requirements of the compressor. It is therefore important to understand how the engine's performance and dynamic operation changes over these various conditions. A simulation procedure was used to analyze the different operating conditions and presents them in a performance map from which an arbitrary operating condition can be inferred. Two maps for heating and cooling operation are shown in Fig. 5. From these figures it can be seen that the working gas mixture and piston amplitude define both power and efficiency for particular charge pressure and temperature conditions. Note that temperature is not used as a primary control for power. As the piston stroke changes, so does the power and as a consequence, the heat input. The burner fuel input is then separately modulated to always keep the head temperature constant within a band of 10 to 20°C.
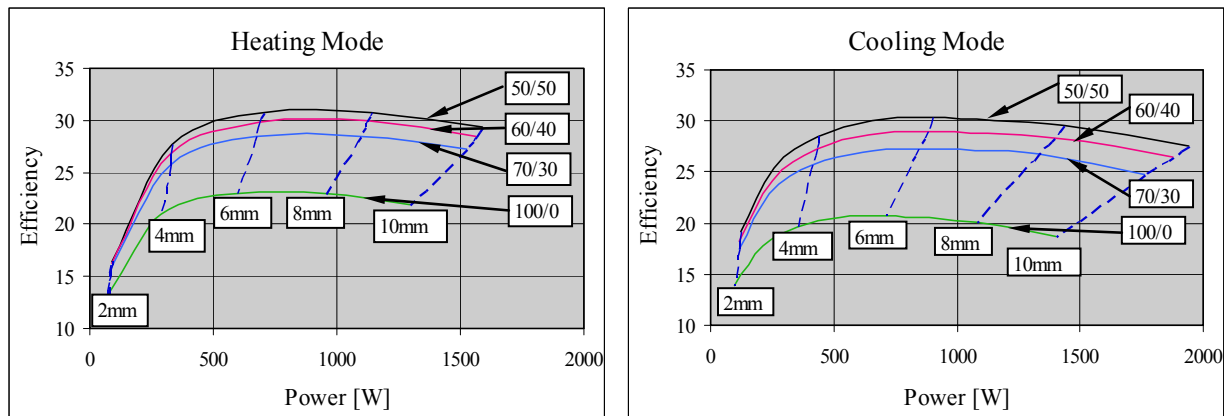
Figure 5: FPSE performance simulation for gas mixture (CO_2/He) and piston amplitude (mm).

3.2 CO_2 Cycle Heat Pump

Compressor efficiency and He separation are discussed for the design condition described in Table 2. An experiment for He separation was conducted using a demonstrative R134a cycle.

3.2.1 Compressor calculation

Compressor swept volume is determined by the requirement of 8 kW evaporation during the heating mode while piston stroke is set by the FPSE operation. This leads to a piston diameter for a given volumetric flow rate. As discussed above, the FPSE frequency varies between 60 and 65 Hz due to the different suction pressure for the heating and cooling mode and during capacity modulation. Compressor performance is generally set by volumetric efficiency, isentropic compression efficiency, and motor efficiency (Rasmussen and Jakobsen 2002). Since the compressor utilizes power directly from the FPSE, the motor efficiency is no longer a concern since it is not an intermediary. However, gas leakage must be accounted for because the dry gas bearings that support the compressor piston are subject to a certain degree of CO_2 leakage across the piston. Since the He–CO_2 mixture of the engine is returned to the compressor buffer space through the return device, He will enter the heat pump cycle and affects the

compressor performance. Therefore, this study considers volumetric efficiency ($\eta_{volumetric}$) and effects due to leakage ($\eta_{leakage}$), friction ($\eta_{friction}$), and He – CO_2 mixture ($\eta_{He\text{-}CO2}$) on the compressor performance.

Table 4 shows the calculated compressor dimensions and efficiency. The volumetric efficiency is relatively high with unusually large top clearance due to a high specific heat ratio and a low pressure ratio for CO_2 gas. The large top clearance allows greater flexibility in the control of the FPSE piston stroke. Leakage across the piston is estimated to be below 1% of the volumetric flow rate of the compressor despite the high -pressure difference of CO_2 cycle. This is achieved by a combination of higher viscosity and a long piston seal. Friction loss is theoretically negligible by virtue of the gas bearing and linear motion, but assumed anyway to be due to no more than 5 N of friction force leading to less than 1% of the required compressor work. He gas circulates by way of a He separation line in the CO_2 cycle and it affects the compressor volumetric efficiency, discharge pressure, and heat transfer in the condenser. The volumetric flow rate of He is the same as the CO_2 leakage rate to the FPSE across the compressor piston because of the CO_2 mole fraction of 0.5 in the FPSE volume. This hurts the compressor volumetric efficiency by the portion of He circulation in the CO_2 cycle. For now the effect of the He mixture on the discharge pressure and heat transfer in the condenser is assumed to be the same proportion as the reduction of volumetric efficiency by He circulation. Other factors such as valve opening and compressor heat transfer losses are accounted for as an efficiency for miscellaneous losses ($\eta_{miscellaneous}$), 0.95.

Table 4: Compressor calculation: dimension and efficiency

Dimensions	Frequency	58 to 66 Hz	
	Piston diameter	23.4 mm	
	Piston stroke	20 mm maxium	
	Piston length	75 mm	
	Top clearance	0.5 mm	
	Radial clearance	0.0075 mm	
Efficiency	$\eta_{volumetric}$	0.988	$= 1 - CL\left[\left(P_{dis}/P_{suc}\right)^{1/\gamma} - 1\right]$
	$\eta_{leakage}$	0.989	= 1-leak rate/volumetric flow rate
	$\eta_{friction}$	0.991	= 1-friction loss/compressor work
	$\eta_{He\text{-}CO2}$	0.978	= 1-(2.0* CO_2 leak rate)/volumetric flow rate
	$\eta_{miscellaneous}$	0.950	= assumed efficiency for miscellaneous losses
	$\eta_{compressor}$	0.900	$= \eta_{volumetric} \cdot \eta_{leakage} \cdot \eta_{friction} \cdot \eta_{He-CO2} \cdot \eta_{miscellaneous}$

3.2.2 He - CO_2 mixture in the heat pump cycle

As mentioned, He existence directly decreases the CO_2 gas volumetric flow for a given compressor swept volume. The discharge pressure is determined by adiabatic compression that depends on a specific heat ratio (γ). The specific heat ratio of the He–CO_2 mixture is similar to CO_2 because that of He is almost the same as CO_2 and the He fraction in the CO_2 cycle is so small. Therefore, the discharge pressure of the He–CO_2 mixture is almost identical to CO_2 only. The heat transfer coefficient in a condenser is similarly affected only slightly due to the small He fraction in the mixture. Since the He separator prevents He gas flowing into the evaporator, the evaporator is not affected at all. Given this, it has been argued that the He–CO_2 mixture affects mainly the volumetric efficiency and to a far lesser degree, the discharge pressure, condenser performance and compressor heat transfer.

The He separator is located at the exit of the condenser after some additional sub-cooling to easily separate He gas from the CO_2, which would be entirely in the liquid state. The separated He gas is returned to the FPSE bounce space as shown in Fig. 1.

3.2.3 Experiment of He separation with a demonstrative R134a cycle

An experiment to study the influence of the He mixture was conducted using a R134a cycle not only because a CO_2 cycle was not available but also for the reason that the process is somewhat independent of

the refrigerant. Expansion valves were placed before and after the He separator so that the pressure at separation could be regulated. Performance comparison was made between a pure R134a cycle and a case where He was added to up to 5% by volume. Pressure at separation was adjusted to investigate its effect on performance. Separated He is returned to the compressor buffer space as shown in Fig. 6, and the suction process circulates it continuously. Evaporation was set to -19°C by an electric wire heater on the evaporator tube. The ambient air temperature of 25°C determined the condensing temperature. R134a was charged for the best cycle match with the test rig (test #1). The limitations of the test rig allowed only relative comparisons to see the effect of He mixture on the Rankine cycle.

Table 5 shows data and test condition. Opening the He separator valve for the normal cycle (test #1) allows R134a vapor to return directly to the compressor buffer space and makes the input power slightly higher (test #2). He addition on top of the R134a pressure was 0.3 bar, which is about 5% of total pressure at room temperature. R134a in the cycle exists in mainly vapor at a room temperature of 25°C. Since the R134a becomes liquid to fill the tubing on the liquid side when the R134a cycle reaches a steady condition, the He volume fraction would be much higher than 5%. This explains the increased discharge pressure with He addition due to the increased specific heat ratio for the He–R134a mixture. The discharge pressure with He addition is almost doubled compared to a normal cycle (test #3). Theoretical adiabatic work for the increased specific heat ratio and pressure ratio is expected to increase by more than 50%. However, the measured input power is increased by 5%. This can be explained by the substantially decreased suction volume of the compressor, caused by the presence of He in the working fluid. The decreased suction volume causes refrigerant flow rate to decrease, and therefore reduces the capacity of evaporation. The evaporation is decreased by 26% compared to the normal cycle.

He was added after test #2. He separation for test #4 and #5 improved the cycle performance by 10% compared to test #3 where the He gas circulated together with R134a through the normal cycle with the He separator closed. The higher the pressure the He separator worked at, the more evaporation the cycle achieved because the He is completely separated and the evaporator is not affected by He circulation. Fig. 6 (right) shows the He separator used in the experiment and the photo was taken during test #5. About 2/3 of internal volume is filled with R134a liquid, and the top 1/3 is filled with He gas flowing to the compressor buffer space. It was observed that all He gas entering the He separator was completely separated and returned to the compressor buffer space.
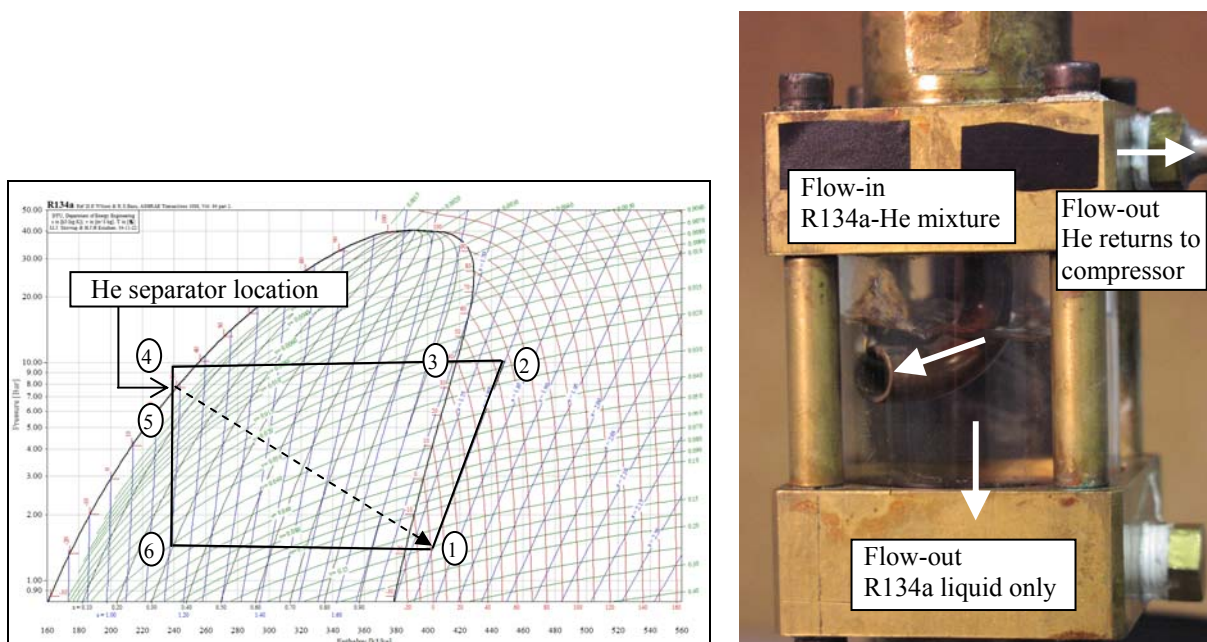
Figure 6: R134a cycle for He separator experiment (left) and
prototype He separator during test #5 showing liquid surface of R134a at working (right)

Table 5: Measured data for R134a cycle with He mixture. Q_{evap} and power in [W]

Test #	Q_{evap}/Power	P_{dis} (2)	$P_{He\text{-}sep}$ (5)	$T_{cond\text{-}in}$ (3)	$T_{cond\,-out}$ (4)	Condition
1	359/295	9.5	7.9	35.0	26.8	R134a, Normal cycle
2	359/300	10.7	5.8	37.4	25.6	R134a+He_sep. open
3	265/310	19.7	7.6	40.1	25.5	R134a+He 0.3bar, Normal
4	282/308	17.7	6.0	43.7	25.2	R134a+He 0.3bar,
5	292/309	17.7	8.1	43.9	24.4	He_sep. open

4 DISCUSSIONS

The system outlined here has been modeled using known and demonstrated component efficiencies. The critical items that determine the practicality of this system are the effects of the working fluid mixture on the engine and heat pump and the stability of the system. These items appear to be manageable by good engineering design. One previous attempt to build a gas fired heat pump based on a free-piston Stirling engine (Marusak and Ackermann 1985) achieved all the performance goals indicated in this study baring the successful coupling to the heat pump. In their case they demonstrated a burner efficiency of between 83 and 85%, an engine efficiency of 32% and excellent durability of the machinery. The heat pump drive was unfortunately crippled by the belief that the working fluid of the engine and heat pump had to be absolutely segregated resulting in a complicated and costly hydraulic drive. If, as has been indicated here, the coupling may be done in a direct manner with due consideration to refrigerant choice and the effects of working fluid leakage, it is clear that a far simpler machine is possible with much higher mechanism efficiencies than has been demonstrated before.

5 CONCLUSIONS

It has been shown that a simple, high-efficiency, residential class, gas fired heat pump is possible and within reach by technologies that are well understood. Excellent PERs are possible in both heating (2.15) and cooling modes (up to 3.34 with water heat capture). The working fluid of the engine runs close to a 50/50 mixture of CO_2 gas and He gas while the heat pump operates with a small volume fraction (below 1%) of He mixed with the CO_2 refrigerant in the compressor and condenser. The He is completely separated from the refrigerant after the condenser (with sub-cooling) so that no He is present in the evaporator. Stability of the system is managed by a linear motor/alternator which also serves as the starting device.

NOMENCLATURE

PER	Primary energy ratio [W/W]	**Subscripts**	
COP	Coefficient of performance [W/W]	suc	suction
EER	Energy efficiency ratio [Btu/h/W]	dis	discharge
CL	Clearance to swept volume ratio	He-sep	He separator
η	Efficiency for compressor design	evap	evaporator
γ	Specific heat ratio, c_p/c_v	cond-in	condenser 1/10 from inlet
P	Pressure [bar]	cond-out	condenser outlet
T	Temperature [°C]		

REFERENCES

Air Condition and Refrigeration Institute, "Standard for ground water-source and ground closed-source heat pumps," *ARI Standard 325/330 & ARI/ASHRAE/ISO 13256-1.*

Berchowitz, D.M. 2004, "Stirling engine driven heat pump with fluid interconnection," *US Patent 6,701,721.*

Bullard, C., Rajan, J. 2004, "Residential space conditioning and water heating with transcritical CO_2 refrigeration cycle," *Proceedings of Int. Refrigeration and Air Conditioning Conference at Purdue.*

Chen, G., McEntee, J. 1993, "Stability criteria and capacity modulation for a free-piston Stirling engine driven linear compressor," *ASME Winter Annual Conference*, New Orleans, Louisiana

Hargreaves, C.M. 1991, *The Philips Stirling Engine*. Elsevier, Amsterdam.

Lane, N.W., Beale, W.T. 1997, "Free-Piston Stirling Design Features," *Proc 8th Int Stirling Engine Conf.*, University of Ancona, Italy.

Lundqvist, Per G. 1993, *Stirling Cycle Heat Pumps and Refrigerators*, doctoral thesis, Royal Inst. Of Technology, Stockholm, Sweden.

Marusak, T.J., Ackermann, R.A. 1985, *Free-Piston Stirling Engine Development*, Gas Research Institute Report 85/0117, Chicago.

MITI, NEDO and Heat Pump Technology Center of Japan 1986, *Proc. Int. Symp. on the Stirling Engine and its Application to Heat Pump Systems, etc.* Heat Pump Technology Center of Japan.

Park, C.Y., Hrnjak, P.S. 2004, "Effect of gas cooler size on its performance and entire R744 A/C system," *Proceedings of Int. Refrigeration and Air Conditioning Conference at Purdue.*

Payne, W.V., B.D., Domanski, P.A. 2001, "A comparison of rating water-source heat pump using ARI Standard 320 and ISO Standard 13256-1," *NISTIR6803*, US Department Of Commerce.

Penswick, L.B., Urieli, I. 1984, "Duplex Stirling machines," *Proc. 19th IECEC*, San Francisco, California, August 1984.

Rasmussen, B.D., Jakobsen, A. 2002, "Review of compressor models and performance characterizing variables," *Proceedings of Int. Compressor Engineering Conference at Purdue.*

Redlich, R.W., Berchowitz, D.M. 1985, "Linear Dynamics of Free-Piston Stirling Engines," *Proc Instn Mech Engrs,* Vol 199, No A3, pp203-213.

Wood, J.G., Unger, R., and Lane, N.W. 2000, "A Stirling-Rankine fuel-fired heat pump," *Int. Compressor Engineering Conference at Purdue*.

Zhang, R.R., Lu, X.S., Li, S.Z., and Gu, A.Z. 2004, "Energy and economic performance comparison of gas engine and electric driven air-to-water heat pump," *Proceedings of Int. Refrigeration and Air Conditioning Conference at Purdue.*

ACKNOWLEDGMENT